Am J Cancer Res 2026;16(5):1791-1804
www.ajcr.us /ISSN:2156-6976/ajcr0170769

Original Article

Reliability of stromal markers multiplex immunofluorescent staining: pathologist assessment compared to quantitative image analysis

Lusine Yaghjyan[1], Yujing J Heng[2], Yaileen D Guzman-Arocho[2], Graham Colditz[3], Brian Sardella[2], Ann Fu[4], Krishna Patel[5], Bernard Rosner[5], Maisey Ratcliffe[1], Rulla M Tamimi[6]

[1]Department of Epidemiology, College of Public Health and Health Professions and College of Medicine, University of Florida, Gainesville, FL, USA; [2]Department of Pathology, Beth Israel Deaconess Medical Center and Harvard Medical School Boston, MA, USA; [3]Division of Public Health Sciences, Washington University School of Medicine in St. Louis, St. Louis, MO, USA; [4]Department of Pathology, Immunology and Laboratory Medicine, College of Medicine, University of Florida, Gainesville, FL, USA; [5]Channing Division of Network Medicine, Department of Medicine, Brigham and Women's Hospital and Harvard Medical School, Boston, MA, USA; [6]Department of Population Health Sciences, Weill Cornell Medicine, New York, NY, USA

Received December 15, 2025; Accepted February 6, 2026; Epub May 15, 2026; Published May 30, 2026

Abstract: Stroma may play an important role in breast carcinogenesis. There is no data on the expression of stromal markers αSMA, FAP, MMP14, TNC, and s100a6 in the breast tissue of cancer-free women. We compared the multiplex immunofluorescence (IF) expression assessment for these markers in normal terminal duct-lobular units (TDLUs) by an expert pathologist with the automated image analysis results and assessed the homogeneity of the markers across multiple cores pertaining to each woman. We included 73 cancer-free women with biopsy-confirmed benign breast disease in the Nurses' Health Study (NHS) and NHSII cohorts. IF was conducted with commercial antibodies (αSMA: 1:400 dilution; FAP: 1:50; MMP14: 1:150; TNC: 1:200; s100a6: 1:300). For each tissue microarray core, the percent positivity was assessed by the pathologist and inForm v2.6.0. Using the pathologist scores as the gold standard, correlations between pathologist and inForm scores were evaluated with Spearman correlation (for categorical positivity: 0, >0 - <1, 1 - 10, >10 - 50, and >50%) and sensitivity/specificity (for binary positivity defined with 1%, 10% and 25% cut-offs). Pathologist and inForm readings were available for 149 and 134 cores, respectively; 105 cores had both. The correlation in the expression across available cores for a woman (median =3, range 1-6) was strong for FAP, MMP14, and s100a6 (Intra-class correlation [ICC]=0.69, 0.72, 0.63, respectively), moderate for αSMA (ICC=0.35), and poor for TNC (ICC=0.21). Correlation between pathologist and inForm was strong for s100a6, FAP, and MMP14 (correlation coefficient =0.77, 0.70, and 0.78, respectively) and moderate for αSMA (0.37) and TNC (0.42). With 1% positivity cut-off, sensitivity was the lowest for TNC (0.30) and ranged between 0.84-0.93 for other markers. Specificity ranged between 0.43-0.98 across all markers with the lowest estimates for αSMA. Sensitivity declined for all markers while using 10% and 25% cut-offs, while specificity increased. Our findings show that computational assessments for αSMA, FAP, MMP14, TNC, and s100a6 exhibit variable correlations with manual assessment. These findings support the use of computational platforms for IF evaluation of most, but not all, stromal markers in large-scale epidemiologic studies and the importance of pilot studies for identification of appropriate cut-offs for defining staining positivity.

Keywords: Stromal cell markers, benign breast disease, automated image analysis, intra-class correlation

Introduction

The human breast is a highly organized, complex organ that consists of an epithelial parenchyma surrounded by stromal cells and extracellular matrix that regulate its proliferation, differentiation, and survival [1]. Emerging evidence suggests that local breast tissue microenvironment and, in particular, stroma, sustain normal tissue structure/function via a variety of signaling mechanisms that control and regulate normal processes and suppress the expression of preneoplastic phenotypes [2-6]. The role of stroma in breast tumor development, progres-

sion, and treatment response, as well as potential utility for targeted therapies, has been widely discussed in recent reviews [7-10]. The resident (normal) fibroblasts are the most abundant stromal cells [6, 11] with a variety of functions, including synthesis/remodeling of extracellular matrix, growth hormone production, tissue repair, angiogenesis, and local immune response via production of chemokines/cytokines [12-17]. However, to date, the evidence of stromal contributions, and particularly the role of normal (resident) fibroblasts, to early stages of carcinogenesis remains unknown due to extremely limited studies with breast tissue from cancer-free women and a lack of evidence on their expression in normal breast tissue. Further, no previous studies have explored the agreement between pathologist manual readings and computer-derived expression of stromal markers, which may have potential implications for large-scale epidemiological studies focusing on stromal contributions to breast carcinogenesis. To address these knowledge gaps, in the current study we aimed to: (1) describe the expression of selected stromal markers in histologically normal breast tissue of cancer-free women; (2) assess the heterogeneity of stromal markers' expression across multiple cores per woman; and (3) compare the immunofluorescent expression assessment for selected stromal markers by an expert pathologist with the results from automated image analysis. The following 5 stromal markers were selected for this study based on their potential utility for breast cancer risk prediction in women with benign breast biospes: alpha-smooth muscle actin (αSMA or ACTA2), fibroblast activation protein (FAP), matrix metallo-peptidase (MMP-14), tenascin-C (TNC), and Calcyclin (s100a6). Understanding the agreement of assessments from automated platforms with pathologist assessments can help in selecting the appropriate analytic method for evaluation of immunoreactivity, particularly in analyses based on archival formalin-fixed paraffin-embedded (FFPE) tissues.

Materials and methods

Study population

Previously established nested case-control study within the Nurses' Health Study (NHS) and Nurses' Health Study II (NHSII) cohorts included cancer-free women with biopsy-confirmed benign breast disease (BBD) who were used for the current analysis [18, 19]. NHS and NHSII prospective cohorts followed registered nurses in the United States who were 30-55 years (NHS) or 25-42 years old (NHSII) at enrollment, respectively. After the initial questionnaire, the data on breast cancer risk factors and any diagnoses of cancer (subsequently confirmed with medical records) or other diseases (including BBD) were updated via biennial questionnaires [20, 21]. This nested case-control study and the assessment of BBD have been described in detail previously [18, 19].

The NHS questionnaires from 1976, 1978, and 1980 asked women whether they had ever been diagnosed with 'fibrocystic disease' or 'other BBD' and whether they had been hospitalized in relation to this diagnosis. Starting in 1982, the NHS questionnaires asked about a history of biopsy-confirmed BBD (fibrocystic disease or other BBD) specifically. The initial NHS II questionnaire from 1989 and all biennial questionnaires also asked women to report any BBD diagnosis and to indicate whether it was confirmed by biopsy or aspiration.

As reported previously [22, 23], cases were defined as women with biopsy-confirmed BBD who later reported a breast cancer diagnosis during 1976-1998 for the NHS and 1989-1999 for the NHSII. Using incidence density sampling, four women with biopsy-confirmed BBD who were cancer-free at the time of the matching case's diagnosis (controls) were matched to the respective case on year of benign breast biopsy and year of birth [24]. Our ability to obtain BBD pathology records and archived biopsy blocks did not significantly differ by case and control status. Women with and without BBD samples had similar distributions of breast cancer risk factors [25]. Our study included a single TMA for 73 women with 222 corresponding tissue cores from normal TDLUs.

The study protocol was approved by the institutional review boards of the Brigham and Women's Hospital and Harvard T.H. Chan School of Public Health, and those of participating registries as required. Consent was obtained or implied by return of questionnaires.

Benign breast biopsy confirmation

The hematoxylin and eosin (H&E) breast tissue slides were retrieved for women providing permission to access their biopsy specimens and were independently reviewed by one of three pathologists who were blinded to the type of BBD noted on the original diagnosis [26, 27]. Any slide with either questionable atypia or atypia was jointly reviewed by two pathologists. Benign breast biopsy was classified in accordance with the categories of Page et al. [28] as non-proliferative, proliferative without atypia, or atypical hyperplasia (ductal or lobular hyperplasia) [18].

Tissue microarray (TMA) construction of BBD samples

Our methods of TMA construction within NHS and NHSII have been previously described [22, 23]. Briefly, H&E sections of the corresponding FFPE tissue blocks were reviewed by a single pathologist to annotate areas of histologically normal terminal duct-lobular units (TDLUs) from which the cores for subsequent TMA construction would be taken [18]. TMAs were constructed at the Dana Farber/Harvard Cancer Center (DF/HCC) Tissue Microarray Core Facility by obtaining 0.6-mm cores from normal TDLUs. Up to 3 cores of normal TDLU for each woman were included in the TMA blocks. Previous evaluation of our TMA construction methods has confirmed a high success rate (76%) of capturing normal TDLUs in these TMA blocks [29]. The current analysis focused specifically on the expression of stromal markers in normal TDLU cores, as normal TDLUs were specifically targeted in the construction of these TMAs within NHS/NHSII and as normal TDLUs were more relevant for future planned studies on contributions of stroma to breast cancer risk focusing on the underlying changes in the breast tissue happening early in the process of breast carcinogenesis.

Multiplex immunofluorescence for stromal markers

In this study, we assessed a single TMA consisting of 222 normal TDLU cores from 73 women. The expression of the stromal markers was evaluated by an automated multiplex immunofluorescence (IF) technique. From a single TMA block, 5-μm paraffin section was cut and then stained with antibodies for αSMA, FAP, MMP14, TNC, and s100a6; an additional marker (cytokeratin, pan Antibody [AE-1/AE-3]) was used to detect epithelial cells for segmentation. The staining was performed at the University of Florida Pathology Core Lab on Leica Bond Autostainer according to the previously standardized protocol with commercial antibodies (αSMA: Abcam, Cambridge, MA, Cat# ab5694, RRID: AB_2223021, 1:400 dilution; FAP: Abcam, Cambridge, MA, Cat# ab207178, RRID: AB_2864720, 1:50 dilution; MMP14, Abcam, Cambridge, MA, Cat# ab-51074, RRID: AB_881234, 1:150 dilution; TNC, Abcam, Cambridge, MA, Cat# ab108930; RRID: AB_10865908, 1:200 dilution; s100a6, Abcam, Cambridge, MA, Cat# ab181975, RRID: AB_3697229, 1:300 dilution; panCK AE1/AE3, Novus Bio, Centennial, CO, Cat# NBP2-29429, RRID: AB_3068002, 1:500 dilution).

Briefly, slides were baked in a 60°C oven for three hours, then deparaffinized and rehydrated using BOND Dewax Solution and Bond Wash Buffer. For heat-induced antigen retrieval, sections were heated at 98°C using Bond ER Solution 1 for 20 minutes. Next, slides were quenched in endogenous peroxidase activity using Peroxide Block (Leica Biosystems, Deer Park, IL). Then slides were rinsed in Bond Wash Buffer and incubated with Opal antibody Diluent/Block (Akoya Biosciences Marlborough, MA) for 10 minutes. Primary antibodies were detected, followed by TSA opal fluorophores (Opal 480, Opal 520, Opal 570, Opal 620, Opal 690, and Opal 780 1:100) for 10 minutes. The slides were counterstained with spectral DAPI (Akoya Bioscience) and were mounted with ProLong Diamond Antifade Mountant (ThermoFisher Scientific, Eugene, OR). The laboratory implemented standard quality control procedures.

Image analysis

The TMA was digitized at 20× using the PhenoImager HT (Akoya Biosciences, Marlborough, MA) using optimized scanning parameters. Immunoreactivity was manually assessed by a board-certified pathologist (YDG) using Phenochart image viewer (Akoya Biosciences). For manual read, the staining extent in stromal regions was quantified as percent of the cells stained positive for each marker out of the stro-

mal area in each core (0 - <1, 1 - <10, 10 - <25, 25 - <50, and ≥50), consistent with our prior assessment of other tissue markers [30-32].

IF was quantified using an automated image analysis software, inForm v2.6.0 (Akoya Biosciences) [33]. The inForm operators (BRS and YJH) selected seven representative tissue cores to train tissue segmentation, ensuring inclusion of cores spanning a range of staining for each of the five stromal markers (Supplementary Data). Auto fluorescence correction for this study utilized a negative control breast cancer tissue section from another Opal multiplex IF study [34] that was re-scanned using this current study's scanning protocol. PanCK and αSMA expression, and the default classifier model in inForm (trainable tissue segmentation with a large-scale pattern of segmentation), was used to train the tissue segmentation to segment each core into epithelial and stromal regions (Supplementary Figure 1). The minimum positive IF threshold was set by referencing the pathologist's manual reads of those seven cores: panCK >0.1, FAP >0.25, TNC >0.25, MMP14 >0.3, αSMA >0.17, and s100a6 >1. These positivity thresholds were optimized through iterative comparison with the pathologist's manual read, ensuring that the minimum threshold used reliably captured marker positivity.

The automated IF quantification (cell-level data across all the detected cores on the TMA) was exported as a.csv file, and further data processing was conducted in R. PanCK+ cells were first excluded as these would be epithelial and myoepithelial cells. Next, αSMA+ cells that were computationally segmented as "epithelial" were excluded as they were likely to be endothelial cells. The remaining cells were considered stromal cells, and their total count per core was used as the denominator for the next calculation. For each core, the extent of each stromal marker's expression was assessed as a continuous % of cells with positive staining (across all intensities) for each marker out of the total number of stromal cells.

Statistical analysis

For analysis, the continuous data from inForm assessment was categorized as 0 - <1, 1 - <10, 10 - <25, 25 - <50, and ≥50, consistent with pathologist assessment. Next, as there is no standardized criteria for defining binary staining positivity for the selected markers, especially in non-malignant breast tissue, and as previous studies utilizing breast tumor tissue used varying criteria [35-40], we used 1%, 10%, and 25%. Distributions of stromal cell markers were presented as numbers and percentages, by staining assessment approach.

Heterogeneity of the stromal cell markers' expression across available cores for a woman was assessed with the intra-class correlation coefficient and 95% Confidence Interval (95% CI), using both continuous as well as categorical expression.

Spearman's rank-ordered correlation coefficients were used to examine the correlation between the pathologist (manual) and inForm marker expression readings. For binary positivity variables with various cut-offs (1%, 10%, and 25%), we calculated sensitivity and specificity, while using pathologist assessment as a gold standard. These correlations, as well as sensitivity and specificity, were also examined while accounting for correlation across available cores for a woman in additional analyses [41].

All analyses were restricted to cores with ≥50 cells from inForm readings, as done previously [22, 42]. The analyses were performed using SAS software (version 9.4, SAS Institute, Cary, NC, USA).

Results

Representative images of IF-stained cores for each of the markers by pathologist-assigned category are shown in **Figure 1**. Among 222 normal TDLU cores in our study, 178 cores had readings from either pathologist or inForm. Pathologist readings were available for 149 cores (67%), and inForm readings were available for 138 cores (62%) for all markers, corresponding to 68 women. Of inForm readings, 4 cores were further excluded from analyses due to low cellularity (cell count <50).

Expression of stromal cell markers in normal TDLUs and heterogeneity across the cores

Distribution of continuous marker expression from automated assessment is presented in **Table 1**. Distribution of categorical expression

	Manual reading score			
Stromal marker	**1 to <10%**	**10 to <25%**	**25 - <50%**	**>50%**
FAP	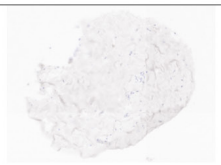	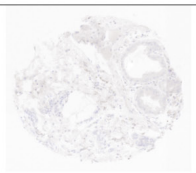	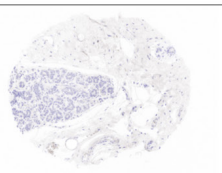	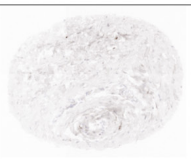
TNC	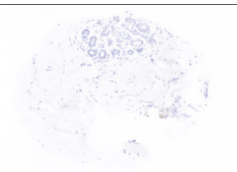	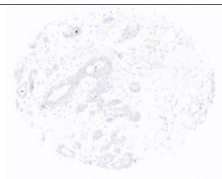	NA	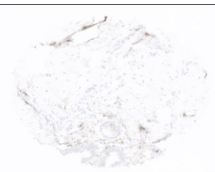
MMP14	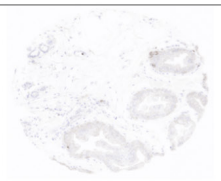	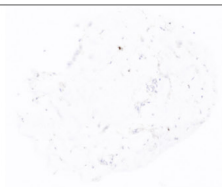	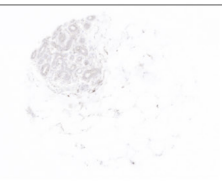	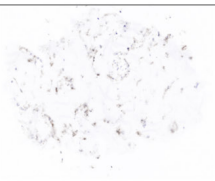
αSMA	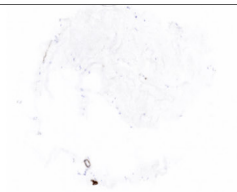	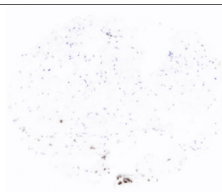	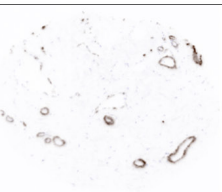	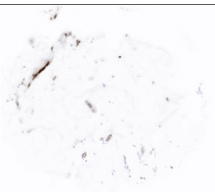
s100a6		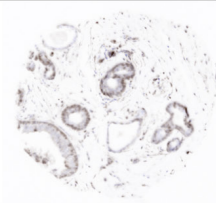	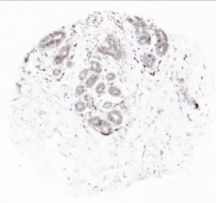	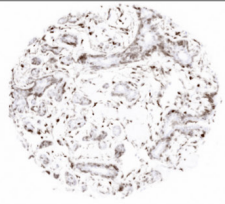

Figure 1. Representative images of stromal markers with ≥1% positivity by pathologist-assigned category. Note: All the images were taken at 10×. To facilitate visualization of tissue architecture, multiplex immunofluorescence images were converted in InForm software to a digital IHC-like representation, whereby individual IF channels are rendered as brown chromogen overlaid on the tissue.

results from pathologist and inForm assessment is presented in **Table 2**. The average number of cores for each woman was 3 (median 3, range 1-6). We found strong correlation in the expression across available cores for a woman for FAP, MMP14, and s100a6, both for continuous expression measures (ICC=0.69, 95% CI 0.54, 0.80; ICC=0.72, 95% CI 0.59, 0.82, and ICC=0.63, 95% CI 0.46, 0.75, respectively) and categorical (ICC=0.67, 95% CI 0.52, 0.78; ICC=0.68, 95% CI 0.53, 0.79, and ICC=0.66, 95% CI 0.51, 0.78, respectively) (**Table 3**).

Table 1. Distribution of continuous marker staining (% positivity) in normal TDLU cores assessed with inForm using a single tissue microarray from Nurses' Health Study and Nurses' Health Study II

Tissue marker/tissue type	N	Mean (SD)	Median	Range
αSMA	134	8.44 (7.46)	7.12	0-55.26
s100a6	134	14.25 (14.95)	7.62	0-60.59
TNC	134	0.45 (1.58)	0.00	0-13.19
FAP	134	14.60 (25.33)	3.98	0-100.00
MMP14	134	10.90 (13.38)	5.49	0-61.81

Abbreviations: αSMA, alpha-smooth muscle actin; FAP, fibroblast activation protein; MMP14, matrix metallo-peptidase; s100a6, calcyclin; SD, standard deviation; TNC, tenascin-C; TDLU, terminal duct lobular unit.

Moderate correlation was observed for αSMA (ICC=0.35 for continuous and ICC=0.38 for categorical expression) and poor correlation was observed for TNC (ICC=0.21 for continuous and 0.00 for categorical expression).

Agreement between pathologist and inForm readings

Of 178 cores with either pathologist or Inform readings, the pathologist and inForm readings were available for 105 cores for all markers. Distribution of continuous inForm readings by the category of manual assessment is presented in **Figure 2**.

Overall percent agreement between manual and inForm scoring was 56% for αSMA, 38% for FAP, 46% for MMP14, 83% for TNC, and 49% for s100a6. We found a strong correlation between pathologist and inForm readings for s100a6 (correlation coefficient r=0.77, 95% CI 0.67; 0.83), FAP (r=0.77, 95% CI 0.59; 0.79), and MMP14 (r=0.78, 95% CI 0.69; 0.85). We found moderate correlations for αSMA (r=0.37, 95% CI 0.20; 0.53) and for TNC (r=0.42, 95% CI 0.26; 0.57) (**Table 4**). These correlations were attenuated after adjustment for correlation across the cores for a woman while using 5 expression categories (Supplemental Table 1).

With 1% positivity cut-off for all markers, sensitivity ranged between 0.84-0.93 for αSMA, s100a6, FAP and MMP14 and was much lower (0.30) for TNC. Sensitivity declined for all markers while using 10% cut-offs (**Table 4**), which was furthermore apparent with the use of 25% cut-offs. Specificity ranged between 0.43-0.98 across all markers, with the lowest estimates for αSMA. The results for sensitivity and specificity remained similar in additional analysis that accounted for correlation across available cores for a woman (Supplementary Table 1).

Discussion

In this study comparing manual pathologist and computer-automated assessments of five stromal markers' expression in cancer-free women with benign breast biopsies, we observed moderate to strong correlations between marker expressions across available cores for a woman for αSMA, FAP, MMP14, and s100a6 and poor correlation for TNC as well as moderate to strong correlation between pathologist and inForm readings for all markers.

The role of stroma in breast tumor development, progression, and treatment response as well as potential utility for targeted therapies has been widely discussed in recent reviews [7-10]. The resident fibroblasts, the most abundant cells [6, 11], have many functions relevant to carcinogenesis [12-17] and play a key role in communicating with surrounding cells during homeostasis and tissue repair [11], modifying breast stem cell activity [43, 44], and extracellular matrix remodeling and cancer growth [45]. However, to date, the evidence of stromal contributions to early stages of carcinogenesis and the expression of stromal markers in normal TDLUs of cancer-free women remains limited. Additionally, there are no established cut-offs for assessment of staining positivity in non-cancerous breast tissue, with various studies in tumors using different cut points [35-40]. In addition, manual assessment of immunoreactivity is semi-quantitative, subjective, labor-intense, and prone to potential bias as the pathologist cannot be blinded with respect to the histology of the evaluated tissue sample. Previous studies with other breast tissue markers in tumor tissue have demonstrated that inter-observer agreement can be influenced by the type of tissue (whole tissue vs. TMA), optical vs. digital microscopy, location of the staining within the cell, and the number and distribu-

Table 2. Distribution of stromal maker expression assessments from Pathologist and inForm readings in normal TDLU cores (N of cores, [%])

Tissue marker	Pathologist (n=149)	inForm (n=134)
αSMA		
Categorical		
0 - <1	13 (8.72)	13 (9.70)
1 - <10	94 (63.09)	84 (62.69)
10 - <25	29 (19.46)	34 (25.37)
25 - <50	12 (8.05)	2 (1.49)
≥50	1 (0.67)	1 (0.75)
Binary, with 1% cut-off		
<1	13 (8.72)	13 (9.70)
≥1	136 (91.28)	121 (90.30)
Binary, with 10% cut-off		
<10	107 (71.81)	97 (72.39
≥10	42 (28.19)	37 (27.61)
Binary, with 25% cut-off		
<25	136 (91.28)	131 (97.76)
≥25	13 (8.72)	3 (2.24)
s100a6		
Categorical		
0 - <1	24 (16.11)	24 (17.91)
1 - <10	32 (21.48)	49 (36.57)
10 - <25	28 (18.79)	27 (20.15)
25 - <50	43 (28.86)	31 (23.13)
≥50	22 (14.77)	3 (2.24)
Binary, with 1% cut-off		
<1	24 (16.11)	24 (17.91)
≥1	125 (83.99)	110 (82.09)
Binary, with 10% cut-off		
<10	56 (37.58)	73 (54.48)
≥10	93 (62.42)	61 (45.52)
Binary, with 25% cut-off		
<25	84 (56.38)	100 (74.63)
≥25	65 (43.62)	34 (25.37)
TNC		
Categorical		
0 - <1	121 (81.21)	123 (91.79)
1 - <10	20 (13.42)	10 (7.46)
10 - <25	4 (2.68)	1 (0.75)
25 - <50	0 (0)	0 (0)
≥50	4 (2.68)	0 (0)
Binary, with 1% cut-off		
<1	121 (81.21)	123 (91.79)
≥1	28 (18.79)	11 (8.21)
Binary, with 10% cut-off		
<10	141 (94.63)	133 (99.25)
≥10	8 (5.37)	1 (0.75)

tion of the cells. In histologically normal tissues, the typically lower levels of the marker expression can further complicate manual assessment and exacerbate observer variability [46-51]. Automated image analysis of TMAs offers a unique opportunity for studying various tissue markers, including stromal markers, in large-scale epidemiological studies by providing objective, reliable, and faster assessment of immunofluorescence results while minimizing pathologist involvement. In this study, we aimed not only to examine the expression of five stromal markers across all available cores for a woman but also to assess the agreement between their expression assessed by a pathologist and by computer-assisted approaches.

Our findings suggest a strong correlation in the expression across available cores for a woman for FAP, MMP14, and s100a6, a moderate correlation for αSMA, and a poor correlation for TNC. Notably, of these five markers, FAP, MMP14, s100a6, and αSMA are localized in cytoplasm, cellular matrix, or nucleus, while TNC is secreted into the extracellular matrix [52] and appears to have the lowest expression levels in normal TDLUs. These biological characteristics may pose technical challenges for both manual and automated assessment of staining positivity, particularly in low-signal contexts, thereby potentially contributing to the reduced concordance observed between the two approaches. Our data demonstrate that despite variability in most of these markers, the correlation across the cores is reasonably high. Though no previous studies examined these correlations, some earlier studies of other markers found strong correlations across available cores (2-3 for a woman) for various other markers [22, 53].

Tissue marker	Pathologist (n=149)	inForm (n=134)
Binary, with 25% cut-off		
<25	145 (97.32)	134 (100.00)
≥25	4 (2.68)	0 (0)
FAP		
Categorical		
0 - <1	25 (16.78)	32 (23.88)
1 - <10	28 (18.79)	57 (42.54)
10 - <25	43 (28.86)	24 (17.91)
25 - <50	26 (17.45)	9 (6.72)
≥50	27 (18.12)	12 (8.96)
Binary, with 1% cut-off		
<1	25 (16.78)	32 (23.88)
≥1	124 (83.22)	102 (76.12)
Binary, with 10% cut-off		
<10	53 (35.57)	89 (66.42)
≥10	96 (64.43)	45 (33.58)
Binary, with 25% cut-off		
<25	96 (64.43)	113 (84.33)
≥25	53 (35.57)	21 (15.67)
MMP14		
Categorical		
0 - <1	29 (19.46)	39 (29.10)
1 - <10	46 (30.87)	42 (31.34)
10 - <25	26 (17.45)	35 (26.12)
25 - <50	25 (16.78)	15 (11.19)
≥50	23 (15.44)	3 (2.24)
Binary, with 1% cut-off		
<1	29 (19.46)	39 (29.10)
≥1	120 (80.54)	95 (70.90)
Binary, with 10% cut-off		
<10	75 (50.34)	81 (60.45)
≥10	74 (49.66)	53 (39.55)
Binary, with 25% cut-off		
<25	101 (67.79)	116 (86.57)
≥25	48 (32.21)	18 (13.43)

Abbreviations: αSMA, alpha-smooth muscle actin; FAP, fibroblast activation protein; MMP14, matrix metallo-peptidase; s100a6, calcyclin; TNC, tenascin-C; TDLU, terminal duct lobular unit.

Table 3. Intra-class correlation (ICC) in marker expression across available cores for a woman as assessed by inForm

Tissue marker	ICC (95% CI) (continuous)	ICC (95% CI) (categorical)
αSMA	0.35 (0.13, 0.54)	0.38 (0.16, 0.56)
s100a6	0.63 (0.46, 0.75)	0.66 (0.51, 0.78)
TNC	0.21 (0.00, 0.43)	0.00 (0.00, 0.22)
FAP	0.69 (0.54, 0.80)	0.67 (0.52, 0.78)
MMP14	0.72 (0.59, 0.82)	0.68 (0.53, 0.79)

Abbreviations: αSMA, alpha-smooth muscle actin; FAP, fibroblast activation protein; MMP14, matrix metallo-peptidase; s100a6, calcyclin; SD, standard deviation; TNC, tenascin-C; TDLU, terminal duct lobular unit.

We found a moderate to strong correlation between the pathologist and inForm assessment. Previous studies have generally shown good agreement between pathologist- and computationally generated scores for a few tumor markers [54-59]. In a recent study of 17 tissue markers in breast tumor tissue from 5,914 NHS and NHSII participants, the correlations between pathologist and computerized assessment using another software, Definiens, ranged from weak to strong and were ≥0.55 for 10 of the 17 examined markers [59]. In our recent reliability study for stem cell markers CD44, CD24, and ALDH1A1, we found moderate to strong correlations [22]. Similar strong correlations were observed by other studies that utilized AQUA algorithms and automated algorithms designed with MatLab for tissue marker evaluation [54, 55, 60, 61] as well as studies that used the Definiens approach in other tumors [62, 63]. However, whether this agreement extends to biomarkers in normal breast TDLUs is unknown. Our findings in histologically normal breast tissue are in line with the previous reports on other markers, though, to our knowledge, stromal markers have not been examined in this capacity in any prior studies.

Our study is the first to date to describe the distribution of αSMA, TNC s100a6, FAP, and MMP14 in normal TDLUs from cancer-free women (including their heterogeneity across the cores for a woman), and to examine the agreement between manual (pathologist) and automated image analysis with inForm. We utilized data and samples from NHS/NHSII cohorts with more than 30 years of follow-up, confirmed benign breast disease, and extensive information on the risk factors for breast cancer. A population-based cohort data allowed us to leverage real-world data

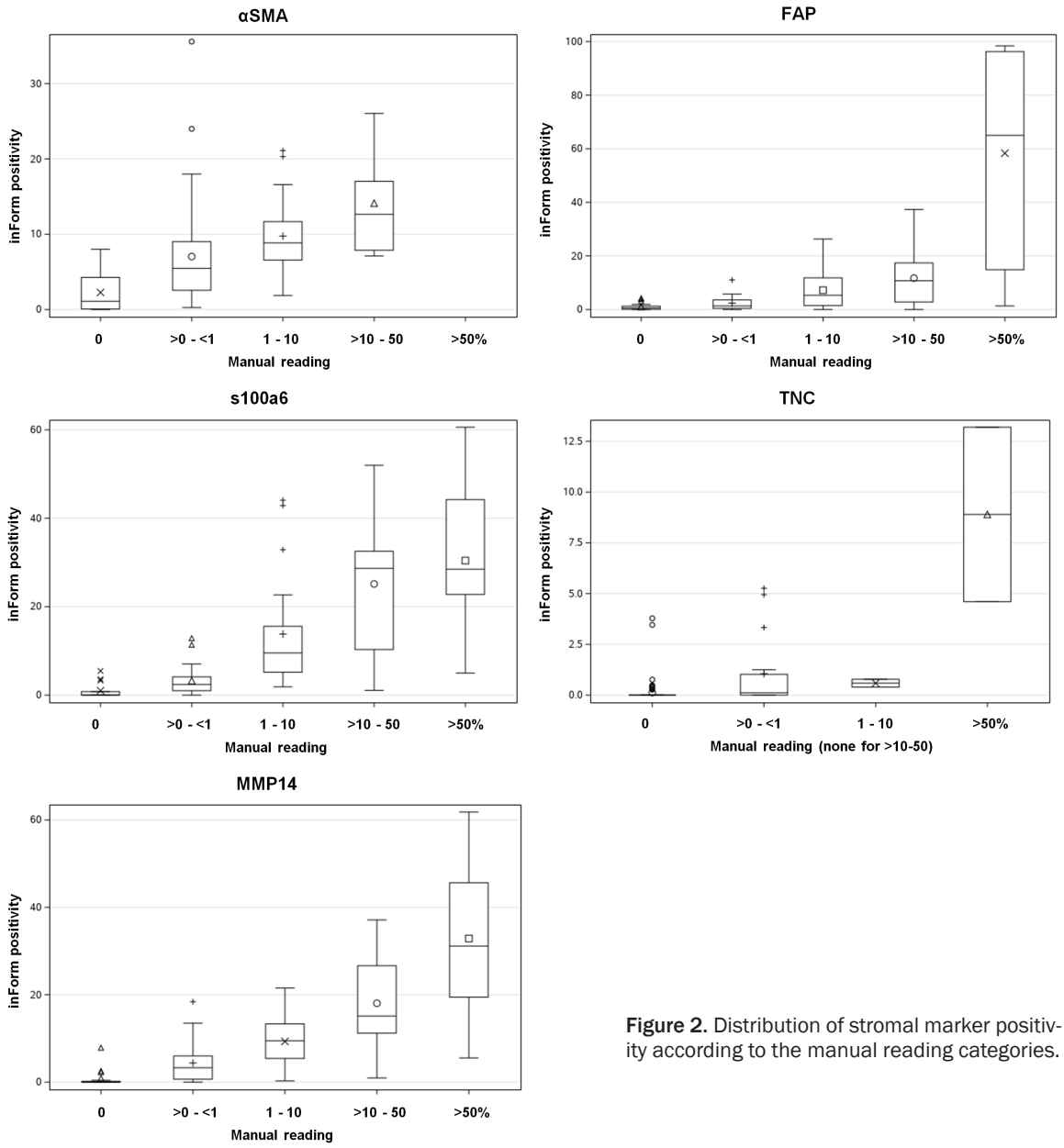

Figure 2. Distribution of stromal marker positivity according to the manual reading categories.

collected from various pathology departments, with different tissue processing protocols, making our results more generalizable to a wider group of researchers. In our study, a single expert pathologist performed all manual readings. We previously reported that quantification of immunoreactivity is highly comparable across various software applications (Definiens, inForm, and QuPath) [33]. The weaker correlation for αSMA is likely due to challenges in assessing αSMA+ stromal cells amongst strongly stained endothelial cells; automated quantification of αSMA+ cells is known to be challenging [64]. The difference in autofluorescence correction may have contributed to the discrepancy in TNC evaluation - Phenochart used by the pathologist to review the slides removes autofluorescence using a built-in pan-tissue filter, while in our inForm workflow, we used a breast tissue negative control to subtract background autofluorescence. Finally, storage time can potentially affect the marker expression levels [65]; however, as we compared pathologist vs. inForm results on a core-by-core basis, the year of sample collection would not affect our findings. Similarly, as test-

Table 4. Correlation of stromal marker expression from Pathologist and inForm assessments in 105 normal TDLU cores (Spearman rank correlation coefficient [95% CI and *p*-value] for categorical classification; sensitivity [95% CI] and specificity [95% CI] for binary variables)

Classification approach	αSMA	s100a6	TNC	FAP	MMP14
Categorical (5 levels)					
Rho (95% CI)	0.37 (0.20; 0.53)	0.77 (0.67; 0.83)	0.43 (0.26; 0.57)	0.70 (0.59; 0.79)	0.78 (0.69; 0.85)
p-value	<0.0001	<0.0001	<0.0001	<0.0001	<0.0001
Binary, 1% cut-off					
Sensitivity	0.93 (0.88; 0.98)	0.92 (0.87; 0.98)	0.30 (0.10; 0.50)	0.84 (0.76; 0.92)	0.84 (0.76; 0.92)
Specificity	0.43 (0.06; 0.80)	0.77 (0.54; 1.00)	0.98 (0.94; 1.00)	0.58 (0.36; 0.80)	0.83 (0.66; 1.00)
Binary, 10% cut-off					
Sensitivity	0.39 (0.22; 0.56)	0.72 (0.61; 0.82)	0.25 (0.00; 0.67)	0.51 (0.40; 0.63)	0.74 (0.62; 0.85)
Specificity	0.84 (0.75; 0.92)	0.95 (0.88; 1.00)	1.00 (1.00; 1.00)	0.97 (0.92; 1.00)	0.90 (0.82; 0.98)
Binary, 25% cut-off					
Sensitivity	0.14 (0.00; 0.40)	0.61 (0.47; 0.75)	NA	0.40 (0.25; 0.55)	0.44 (0.27; 0.61)
Specificity	0.99 (0.97; 1.00)	0.95 (0.89; 1.00)	NA	0.98 (0.95; 1.00)	1.00 (1.00; 1.00)

Abbreviations: αSMA, alpha-smooth muscle actin; CI, confidence interval; FAP, fibroblast activation protein; MMP14, matrix metallo-peptidase; NA, not available (no observations with TNC inForm score >25%); s100a6, calcyclin; TNC, tenascin-C; TDLU, terminal duct lobular units.

ing heterogeneity across the cores is based on the cores that were obtained from the same biopsy sample (i.e., biopsy year), these findings also would not be affected by the biopsy year.

In conclusion, we described the expression of αSMA, s100a6, TNC, FAP, and MMP14 in normal TDLUs of cancer-free women and compared immunoreactivity assessment by pathologist and computational approach. Our data indicate that, despite sufficient variability in the expression of selected stromal markers, the correlation across the cores for a woman is reasonably high for most of the markers. Our findings show that inForm semi-automated digital image analysis can provide results that are comparable to those obtained by an expert pathologist for these stromal markers, and that cut points for computationally derived data may require marker-specific optimization. Importantly, any large-scale investigations would benefit from pilot studies beforehand to improve agreement with pathologist's evaluations prior to wider study implementation.

Acknowledgements

This work was supported by the National Cancer Institute at the National Institutes of Health [CA277817, CA240341 to L.Y., CA131332, CA175080, P01 CA087969 to R.M.T., UM1 CA186107 to M.S., U01 CA176726 to W.W], Avon Foundation for Women, Susan G. Komen for the Cure®, and Breast Cancer Research Foundation.

The authors would like to acknowledge the contribution to this study from central cancer registries supported through the Centers for Disease Control and Prevention's National Program of Cancer Registries (NPCR) and/or the National Cancer Institute's Surveillance, Epidemiology, and End Results (SEER) Program. Central registries may also be supported by state agencies, universities, and cancer centers. Participating central cancer registries include the following: Alabama, Alaska, Arizona, Arkansas, California, Colorado, Connecticut, Delaware, Florida, Georgia, Hawaii, Idaho, Indiana, Iowa, Kentucky, Louisiana, Massachusetts, Maine, Maryland, Michigan, Mississippi, Montana, Nebraska, Nevada, New Hampshire, New Jersey, New Mexico, New York, North Carolina, North Dakota, Ohio, Oklahoma, Oregon, Pennsylvania, Puerto Rico, Rhode Island, Seattle SEER Registry, South Carolina, Tennessee, Texas, Utah, Virginia, West Virginia, Wyoming.

Disclosure of conflict of interest

None.

Address correspondence to: Dr. Lusine Yaghjyan, Department of Epidemiology, College of Public Health and Health Professions and College of Medicine, University of Florida, 2004 Mowry Road, Gainesville, FL 32610, USA. Tel: 352-294-5940; ORCID: 0000-0002-1626-5340; Fax: 352-273-5365; E-mail: lyaghjyan@ufl.edu

References

[1] Arendt LM, Rudnick JA, Keller PJ and Kuperwasser C. Stroma in breast development and disease. Semin Cell Dev Biol 2010; 21: 11-18.

[2] Conklin MW and Keely PJ. Why the stroma matters in breast cancer: insights into breast cancer patient outcomes through the examination of stromal biomarkers. Cell Adh Migr 2012; 6: 249-260.

[3] Barcellos-Hoff MH and Medina D. New highlights on stroma-epithelial interactions in breast cancer. Breast Cancer Res 2005; 7: 33-36.

[4] Nazari SS and Mukherjee P. An overview of mammographic density and its association with breast cancer. Breast Cancer 2018; 25: 259-267.

[5] Kim JB, Stein R and O'Hare MJ. Tumour-stromal interactions in breast cancer: the role of stroma in tumourigenesis. Tumor Biology 2005; 26: 173-185.

[6] Buchsbaum RJ and Oh SY. Breast cancer-associated fibroblasts: where we are and where we need to go. Cancers (Basel) 2016; 8: 19.

[7] Bussard KM, Mutkus L, Stumpf K, Gomez-Manzano C and Marini FC. Tumor-associated stromal cells as key contributors to the tumor microenvironment. Breast Cancer Res 2016; 18: 84.

[8] Angelucci C, Maulucci G, Lama G, Proietti G, Colabianchi A, Papi M, Maiorana A, De Spirito M, Micera A, Balzamino OB, Di Leone A, Masetti R and Sica G. Epithelial-stromal interactions in human breast cancer: effects on adhesion, plasma membrane fluidity and migration speed and directness. PLoS One 2012; 7: e50804-e50804.

[9] Dykes SS, Hughes VS, Wiggins JM, Fasanya HO, Tanaka M and Siemann D. Stromal cells in breast cancer as a potential therapeutic target. Oncotarget 2018; 9: 23761-23779.

[10] McCuaig R, Wu F, Dunn J, Rao S and Dahlstrom JE. The biological and clinical significance of stromal-epithelial interactions in breast cancer. Pathology 2017; 49: 133-140.

[11] Sahai E, Astsaturov I, Cukierman E, DeNardo DG, Egeblad M, Evans RM, Fearon D, Greten FR, Hingorani SR, Hunter T, Hynes RO, Jain RK, Janowitz T, Jorgensen C, Kimmelman AC, Kolonin MG, Maki RG, Powers RS, Puré E, Ramirez DC, Scherz-Shouval R, Sherman MH, Stewart S, Tlsty TD, Tuveson DA, Watt FM, Weaver V, Weeraratna AT and Werb Z. A framework for advancing our understanding of cancer-associated fibroblasts. Nat Rev Cancer 2020; 20: 174-186.

[12] Fukumura D, Xavier R, Sugiura T, Chen Y, Park EC, Lu N, Selig M, Nielsen G, Taksir T, Jain RK and Seed B. Tumor induction of VEGF promoter activity in stromal cells. Cell 1998; 94: 715-725.

[13] Kraman M, Bambrough PJ, Arnold JN, Roberts EW, Magiera L, Jones JO, Gopinathan A, Tuveson DA and Fearon DT. Suppression of antitumor immunity by stromal cells expressing fibroblast activation protein-alpha. Science 2010; 330: 827-830.

[14] Buechler MB and Turley SJ. A short field guide to fibroblast function in immunity. Semin Immunol 2018; 35: 48-58.

[15] Wang LC, Lo A, Scholler J, Sun J, Majumdar RS, Kapoor V, Antzis M, Cotner CE, Johnson LA, Durham AC, Solomides CC, June CH, Puré E and Albelda SM. Targeting fibroblast activation protein in tumor stroma with chimeric antigen receptor T cells can inhibit tumor growth and augment host immunity without severe toxicity. Cancer Immunol Res 2014; 2: 154-166.

[16] Philippeos C, Telerman SB, Oulès B, Pisco AO, Shaw TJ, Elgueta R, Lombardi G, Driskell RR, Soldin M, Lynch MD and Watt FM. Spatial and single-cell transcriptional profiling identifies functionally distinct human dermal fibroblast subpopulations. J Invest Dermatol 2018; 138: 811-825.

[17] Biffi G, Oni TE, Spielman B, Hao Y, Elyada E, Park Y, Preall J and Tuveson DA. IL1-induced JAK/STAT signaling is antagonized by TGFβ to shape CAF heterogeneity in pancreatic ductal adenocarcinoma. Cancer Discov 2019; 9: 282-301.

[18] Tamimi RM, Colditz GA, Wang Y, Collins LC, Hu R, Rosner B, Irie HY, Connolly JL and Schnitt SJ. Expression of IGF1R in normal breast tissue and subsequent risk of breast cancer. Breast Cancer Res Treat 2011; 128: 243-250.

[19] Collins LC, Baer HJ, Tamimi RM, Connolly JL, Colditz GA and Schnitt SJ. The influence of family history on breast cancer risk in women with biopsy-confirmed benign breast disease: results from the Nurses' Health Study. Cancer 2006; 107: 1240-1247.

[20] Tamimi RM, Byrne C, Colditz GA and Hankinson SE. Endogenous hormone levels, mammographic density, and subsequent risk of breast cancer in postmenopausal women. J Natl Cancer Inst 2007; 99: 1178-1187.

[21] Vachon CM, Kuni CC, Anderson K, Anderson VE and Sellers TA. Association of mammographically defined percent breast density with epidemiologic risk factors for breast cancer (United States). Cancer Causes Control 2000; 11: 653-662.

[22] Yaghjyan L, Heng YJ, Baker GM, Bret-Mounet V, Murthy D, Mahoney MB, Mu Y, Rosner B and Tamimi RM. Reliability of CD44, CD24, and ALDH1A1 immunohistochemical staining: pathol-

ogist assessment compared to quantitative image analysis. Front Med (Lausanne) 2022; 9: 1040061.
[23] Yaghjyan L, Heng YJ, Baker GM, Murthy D, Mahoney MB, Rosner B and Tamimi RM. Associations of stem cell markers in benign breast tissue with subsequent breast cancer risk. Am J Cancer Res 2023; 13: 6280-6289.
[24] Tamimi RM, Rosner B and Colditz GA. Evaluation of a breast cancer risk prediction model expanded to include category of prior benign breast disease lesion. Cancer 2010; 116: 4944-4953.
[25] Kensler KH, Beca F, Baker GM, Heng YJ, Beck AH, Schnitt SJ, Hazra A, Rosner BA, Eliassen AH, Hankinson SE, Brown M and Tamimi RM. Androgen receptor expression in normal breast tissue and subsequent breast cancer risk. NPJ Breast Cancer 2018; 4: 33.
[26] Jacobs TW, Byrne C, Colditz G, Connolly JL and Schnitt SJ. Pathologic features of breast cancers in women with previous benign breast disease. Am J Clin Pathol 2001; 115: 362-369.
[27] Tamimi RM, Byrne C, Baer HJ, Rosner B, Schnitt SJ, Connolly JL and Colditz GA. Benign breast disease, recent alcohol consumption, and risk of breast cancer: a nested case-control study. Breast Cancer Res 2005; 7: R555-62.
[28] Page DL, Dupont WD, Rogers LW and Rados MS. Atypical hyperplastic lesions of the female breast. A long-term follow-up study. Cancer 1985; 55: 2698-2708.
[29] Collins LC, Wang YH, Connolly JL, Baer HJ, Hu R, Schnitt SJ, Colditz GA and Tamimi RM. Potential role of tissue microarrays for the study of biomarker expression in benign breast disease and normal breast tissue. Appl Immunohistochem Mol Morphol 2009; 17: 438-441.
[30] Lee JH, Bae SB, Oh MH, Cho HD, Jang SH, Hong SA, Cho J, Kim SY, Han SW, Lee JE, Kim HJ and Lee HJ. Clinicopathologic and prognostic significance of transducin-like enhancer of split 1 protein expression in invasive breast cancer. J Breast Cancer 2017; 20: 45-53.
[31] Lakhani SR, Reis-Filho JS, Fulford L, Penault-Llorca F, van der Vijver M, Parry S, Bishop T, Benitez J, Rivas C, Bignon YJ, Chang-Claude J, Hamann U, Cornelisse CJ, Devilee P, Beckmann MW, Nestle-Krämling C, Daly PA, Haites N, Varley J, Lalloo F, Evans G, Maugard C, Meijers-Heijboer H, Klijn JG, Olah E, Gusterson BA, Pilotti S, Radice P, Scherneck S, Sobol H, Jacquemier J, Wagner T, Peto J, Stratton MR, McGuffog L and Easton DF; Breast Cancer Linkage Consortium. Prediction of BRCA1 status in patients with breast cancer using estrogen receptor and basal phenotype. Clin Cancer Res 2005; 11: 5175-5180.
[32] Hanna M, Dumas I, Orain M, Jacob S, Têtu B, Sanschagrin F, Bureau A, Poirier B and Diorio C. Association between local inflammation and breast tissue age-related lobular involution among premenopausal and postmenopausal breast cancer patients. PLoS One 2017; 12: e0183579.
[33] Baker GM, Bret-Mounet VC, Wang T, Veta M, Zheng H, Collins LC, Eliassen AH, Tamimi RM and Heng YJ. Immunohistochemistry scoring of breast tumor tissue microarrays: a comparison study across three software applications. J Pathol Inform 2022; 13: 100118.
[34] Baker GM, Bret-Mounet VC, Xu J, Fein-Zachary VJ, Tobias AM, Bartlett RA, Clohessy JG, Vlachos IS, Massicott ES, Wulf GM, Schnitt SJ and Heng YJ. Toker cell hyperplasia in the nipple-areolar complex of transmasculine individuals. Mod Pathol 2023; 36: 100121.
[35] Abdallah DM and Deeb NMFE. Comparative immunohistochemical study of P63, SMA, CD10 and calponin in distinguishing in situ from invasive breast carcinoma. Journal of Molecular Biomarkers & Diagnosis 2017; 8: 1-4.
[36] Catteau X, Simon P, Vanhaeverbeek M and Noël JC. Variable stromal periductular expression of CD34 and smooth muscle actin (SMA) in intraductal carcinoma of the breast. PLoS One 2013; 8: e57773.
[37] Tse GM, Tan PH, Lui PC, Gilks CB, Poon CS, Ma TK, Law BK and Lam WW. The role of immunohistochemistry for smooth-muscle actin, p63, CD10 and cytokeratin 14 in the differential diagnosis of papillary lesions of the breast. J Clin Pathol 2007; 60: 315-320.
[38] Köhrmann A, Kammerer U, Kapp M, Dietl J and Anacker J. Expression of matrix metalloproteinases (MMPs) in primary human breast cancer and breast cancer cell lines: new findings and review of the literature. BMC Cancer 2009; 9: 188-188.
[39] Kim HM, Lee YK and Koo JS. Expression of CAF-related proteins is associated with histologic grade of breast phyllodes tumor. Dis Markers 2016; 2016: 4218989.
[40] Vizoso FJ, González LO, Corte MD, Rodríguez JC, Vázquez J, Lamelas ML, Junquera S, Merino AM and García-Muñiz JL. Study of matrix metalloproteinases and their inhibitors in breast cancer. Br J Cancer 2007; 96: 903-911.
[41] Rosner B and Glynn RJ. Interval estimation for rank correlation coefficients based on the probit transformation with extension to measurement error correction of correlated ranked data. Stat Med 2007; 26: 633-646.
[42] Turashvili G, Leung S, Turbin D, Montgomery K, Gilks B, West R, Carrier M, Huntsman D and Aparicio S. Inter-observer reproducibility of

HER2 immunohistochemical assessment and concordance with fluorescent in situ hybridization (FISH): pathologist assessment compared to quantitative image analysis. BMC cancer 2009; 9: 165-165.
[43] Brizzi MF, Tarone G and Defilippi P. Extracellular matrix, integrins, and growth factors as tailors of the stem cell niche. Curr Opin Cell Biol 2012; 24: 645-651.
[44] Le Guen L, Marchal S, Faure S and de Santa Barbara P. Mesenchymal-epithelial interactions during digestive tract development and epithelial stem cell regeneration. Cell Mol Life Sci 2015; 72: 3883-3896.
[45] Avagliano A, Fiume G, Ruocco MR, Martucci N, Vecchio E, Insabato L, Russo D, Accurso A, Masone S, Montagnani S and Arcucci A. Influence of fibroblasts on mammary gland development, breast cancer microenvironment remodeling, and cancer cell dissemination. Cancers 2020; 12: 1697.
[46] Baez-Navarro X, van Bockstal MR, Nawawi D, Broeckx G, Colpaert C, Doebar SC, Hogenes MCH, Koop E, Lambein K, Peeters DJE, Sinke RHJA, Bastiaan van Brakel J, van der Starre-Gaal J, van der Vegt B, van de Vijver K, Vreuls CPH, Vreuls W, Westenend PJ and van Deurzen CHM. Interobserver variation in the assessment of immunohistochemistry expression levels in HER2-negative breast cancer: can we improve the identification of low levels of HER2 expression by adjusting the criteria? An international interobserver study. Mod Pathol 2023; 36: 100009.
[47] Gavrielides MA, Conway C, O'Flaherty N, Gallas BD and Hewitt SM. Observer performance in the use of digital and optical microscopy for the interpretation of tissue-based biomarkers. Anal Cell Pathol (Amst) 2014; 2014: 157308.
[48] Meyerholz DK and Beck AP. Principles and approaches for reproducible scoring of tissue stains in research. Lab Invest 2018; 98: 844-855.
[49] Callau C, Lejeune M, Korzynska A, García M, Bueno G, Bosch R, Jaén J, Orero G, Salvadó T and López C. Evaluation of cytokeratin-19 in breast cancer tissue samples: a comparison of automatic and manual evaluations of scanned tissue microarray cylinders. Biomed Eng Online 2015; 14 Suppl 2: S2.
[50] Stålhammar G, Fuentes Martinez N, Lippert M, Tobin NP, Mølholm I, Kis L, Rosin G, Rantalainen M, Pedersen L, Bergh J, Grunkin M and Hartman J. Digital image analysis outperforms manual biomarker assessment in breast cancer. Mod Pathol 2016; 29: 318-329.
[51] Bernhardt M, Weinhold L, Sanders C, Hommerding O, Lau JF, Toma M, Tischler V, Schmid M, Zienkiewicz T, Hildenbrand R, Gerlach P, Zhou H, Braun M, Müller G, Sieber E, Marko C and Kristiansen G. Peer-to-peer validation of Ki-67 scoring in a pathology quality circle as a tool to assess interobserver variability: are we better than we thought? Apmis 2024; 132: 718-727.
[52] Chiquet-Ehrismann R and Tucker RP. Tenascins and the importance of adhesion modulation. Cold Spring Harb Perspect Biol 2011; 3: a004960.
[53] Yaghjyan L, Esnakula AK, Scott CG, Wijayabahu AT, Jensen MR and Vachon CM. Associations of mammographic breast density with breast stem cell marker-defined breast cancer subtypes. Cancer Causes Control 2019; 30: 1103-1111.
[54] Camp RL, Chung GG and Rimm DL. Automated subcellular localization and quantification of protein expression in tissue microarrays. Nat Med 2002; 8: 1323-1327.
[55] Rexhepaj E, Brennan DJ, Holloway P, Kay EW, McCann AH, Landberg G, Duffy MJ, Jirstrom K and Gallagher WM. Novel image analysis approach for quantifying expression of nuclear proteins assessed by immunohistochemistry: application to measurement of oestrogen and progesterone receptor levels in breast cancer. Breast Cancer Res 2008; 10: R89.
[56] Turbin DA, Leung S, Cheang MC, Kennecke HA, Montgomery KD, McKinney S, Treaba DO, Boyd N, Goldstein LC, Badve S, Gown AM, van de Rijn M, Nielsen TO, Gilks CB and Huntsman DG. Automated quantitative analysis of estrogen receptor expression in breast carcinoma does not differ from expert pathologist scoring: a tissue microarray study of 3,484 cases. Breast Cancer Res Treat 2008; 110: 417-426.
[57] Diaz LK, Sahin A and Sneige N. Interobserver agreement for estrogen receptor immunohistochemical analysis in breast cancer: a comparison of manual and computer-assisted scoring methods. Ann Diagn Pathol 2004; 8: 23-27.
[58] Lehr HA, Jacobs TW, Yaziji H, Schnitt SJ and Gown AM. Quantitative evaluation of HER-2/neu status in breast cancer by fluorescence in situ hybridization and by immunohistochemistry with image analysis. Am J Clin Pathol 2001; 115: 814-822.
[59] Roberts MR, Baker GM, Heng YJ, Pyle ME, Astone K, Rosner BA, Collins LC, Eliassen AH and Tamimi RM. Reliability of a computational platform as a surrogate for manually interpreted immunohistochemical markers in breast tumor tissue microarrays. Cancer Epidemiol 2021; 74: 101999.
[60] Howat WJ, Blows FM, Provenzano E, Brook MN, Morris L, Gazinska P, Johnson N, McDuffus LA, Miller J, Sawyer EJ, Pinder S, van Deurzen CH,

Jones L, Sironen R, Visscher D, Caldas C, Daley F, Coulson P, Broeks A, Sanders J, Wesseling J, Nevanlinna H, Fagerholm R, Blomqvist C, Heikkilä P, Ali HR, Dawson SJ, Figueroa J, Lissowska J, Brinton L, Mannermaa A, Kataja V, Kosma VM, Cox A, Brock IW, Cross SS, Reed MW, Couch FJ, Olson JE, Devillee P, Mesker WE, Seyaneve CM, Hollestelle A, Benitez J, Perez JI, Menéndez P, Bolla MK, Easton DF, Schmidt MK, Pharoah PD, Sherman ME and García-Closas M. Performance of automated scoring of ER, PR, HER2, CK5/6 and EGFR in breast cancer tissue microarrays in the Breast Cancer Association Consortium. J Pathol Clin Res 2014; 1: 18-32.

[61] Bankhead P, Fernández JA, McArt DG, Boyle DP, Li G, Loughrey MB, Irwin GW, Harkin DP, James JA, McQuaid S, Salto-Tellez M and Hamilton PW. Integrated tumor identification and automated scoring minimizes pathologist involvement and provides new insights to key biomarkers in breast cancer. Lab Invest 2018; 98: 15-26.

[62] Braun M, Kirsten R, Rupp NJ, Moch H, Fend F, Wernert N, Kristiansen G and Perner S. Quantification of protein expression in cells and cellular subcompartments on immunohistochemical sections using a computer supported image analysis system. Histol Histopathol 2013; 28: 605-610.

[63] Feuchtinger A, Stiehler T, Jütting U, Marjanovic G, Luber B, Langer R and Walch A. Image analysis of immunohistochemistry is superior to visual scoring as shown for patient outcome of esophageal adenocarcinoma. Histochem Cell Biol 2015; 143: 1-9.

[64] Hillsley A, Santos JE and Rosales AM. A deep learning approach to identify and segment alpha-smooth muscle actin stress fiber positive cells. Sci Rep 2021; 11: 21855.

[65] Blows FM, Ali HR, Dawson SJ, Le Quesne J, Provenzano E, Caldas C and Pharoah PD. Decline in antigenicity of tumor markers by storage time using pathology sections cut from tissue microarrays. Appl Immunohistochem Mol Morphol 2016; 24: 221-226.

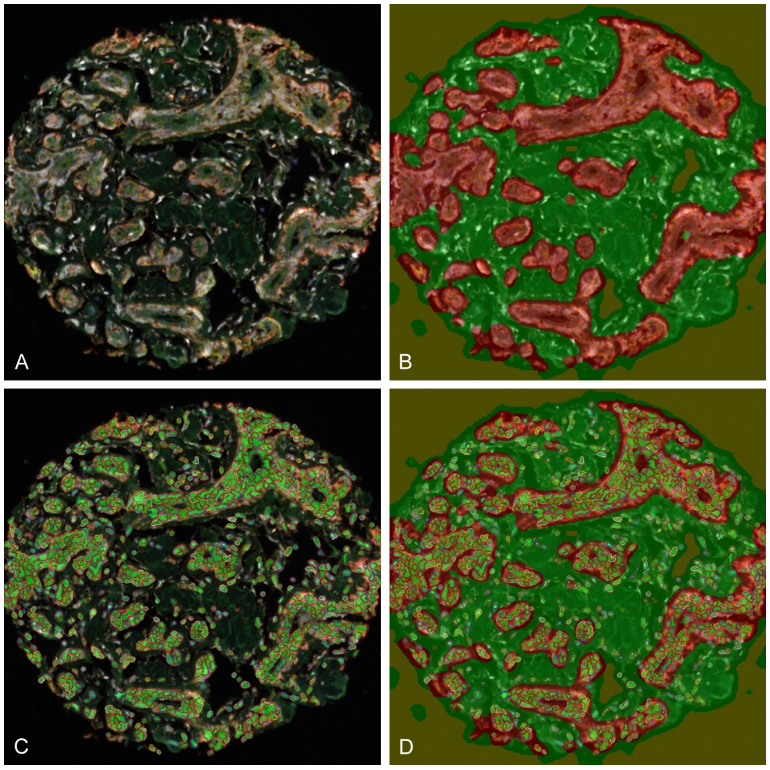

Supplementary Figure 1. inForm analysis pipeline demonstrating segmentation of epithelial vs. stromal regions. A. A representative breast tissue core stained for FAP (Opal 480, cyan), tenascin (Opal 520, green), panCK (Opal 570, yellow), MMP14 (Opal 620, orange), a-SMA (Opal 690, red) and S1006A (Opal 780, white). Autofluorescence has been removed. B. The operator trains the tissue segmentation algorithm. Tissue is segmented into epithelium/endothelium (red overlay), fibrous stroma (green), and background (yellow). C. Automated cell detection is carried out by applying color thresholding for the nuclear stain (DAPI). Detected nuclei are indicated in neon green. D. Integrating positive cell detection and tissue segmentation allows for specific analysis of cells and staining in the fibrous stroma.

Supplementary Table 1. Correlation of stromal marker expression in 105 normal TDLU cores from Pathologist and inForm assessments, accounting for correlation across available cores for a woman (Spearman rank correlation coefficient [95% CI and *p*-value] for categorical; sensitivity [95% CI] and specificity [95% CI] for binary variables)

Modeling approach	αSMA	s100a6	TNC	FAP	MMP14
Categorical (5 levels)					
Rho (95% CI)	0.14 (-0.18, 0.43)	0.53 (0.12, 0.79)	0.28 (0.02, 0.50)	0.51 (0.26, 0.69)	0.54 (0.19, 0.77)
p-value	0.43	0.053	0.071	0.004	0.029
Binary, 1% as cut-off					
Sensitivity	0.93 (0.83, 0.97)	0.92 (0.81, 0.97)	0.32 (0.16, 0.53)	0.83 (0.71, 0.91)	0.85 (0.71, 0.93)
Specificity	0.43 (0.14, 0.77)	0.77 (0.44, 0.93)	0.98 (0.91, 0.99)	0.58 (0.35, 0.78)	0.83 (0.50, 0.96)
Binary, as 10% cut-off					
Sensitivity	0.39 (0.22, 0.59)	0.72 (0.56, 0.84)	0.25 (0.05, 0.68)	0.52 (0.37, 0.67)	0.75 (0.62, 0.85)
Specificity	0.83 (0.72, 0.91)	0.94 (0.80, 0.99)	N/A	0.97 (0.82, 1.00)	0.92 (0.80, 0.97)
Binary, as 25% cut-off					
Sensitivity	0.14 (0.02, 0.58)	0.61 (0.43, 0.76)	N/A	0.40 (0.22, 0.61)	0.45 (0.33, 0.59)
Specificity	0.99 (0.93,1.00)	0.95 (0.85, 0.98)	N/A	0.98 (0.90, 1.00)	N/A

Abbreviations: αSMA, alpha-smooth muscle actin; CI, confidence interval; FAP, fibroblast activation protein; MMP14, matrix metallo-peptidase; NA, not available (no observations with TNC inForm score >25%); s100a6, calcyclin; TNC, tenascin-C; TDLU, terminal duct lobular units.